Neurobiology of Aging 80 (2019) 187–195

Contents lists available at ScienceDirect

Neurobiology of Aging

journal homepage: www.elsevier.com/locate/neuaging

An analog derived from phenylpropanoids ameliorates Alzheimer's disease–like pathology and protects mitochondrial function

Shichao Huang [a,1], Xin Cao [b,1], Yue Zhou [a], Fuchun Shi [c], Shunmei Xin [a], Shufang He [d], Yuqian An [a,e], Longfei Gao [a,e], Yongfeng Yang [a,e], Biao Yu [c,*], Gang Pei [a,f,g,**]

[a] State Key Laboratory of Cell Biology, Institute of Biochemistry and Cell Biology, Shanghai Institutes for Biological Sciences, Chinese Academy of Sciences, Shanghai, China
[b] Zhongshan Institute of Clinical Science, Fudan University, Shanghai, China
[c] State Key Laboratory of Bioorganic and Natural Products Chemistry, Center for Excellence in Molecular Synthesis, Shanghai Institute of Organic Chemistry, Chinese Academy of Sciences, Shanghai, China
[d] National Center for Protein Science Shanghai, Shanghai Institute of Biochemistry and Cell Biology, Chinese Academy of Sciences, Shanghai, China
[e] Graduate School, University of Chinese Academy of Sciences, Chinese Academy of Sciences, Shanghai, China
[f] Shanghai Key Laboratory of Signaling and Disease Research, Laboratory of Receptor-based Biomedicine, The Collaborative Innovation Center for Brain Science, School of Life Sciences and Technology, Tongji University, Shanghai, China
[g] Institute for Stem Cell and Regeneration, Chinese Academy of Sciences, Beijing, China

ARTICLE INFO

Article history:
Received 18 June 2018
Received in revised form 23 April 2019
Accepted 1 May 2019
Available online 9 May 2019

Keywords:
Alzheimer's disease
Neural progenitor cell proliferation
Neurogenesis
Mitochondrial dysfunction
Natural products
AMPK

ABSTRACT

The abnormal proliferation and neurogenesis of neural progenitor cells (NPCs) is usually associated with the pathophysiology of neurodegenerative disorders such as Alzheimer's disease (AD). Mitochondrial stress is one of the most prominent features of AD and is thought to be involved in the impairment of the neurogenesis and proliferation of NPCs. Thus, restoring mitochondrial function by pharmaceutical intervention may alleviate disease-related defects in neurogenesis and is considered a potential therapeutic strategy for AD. In the present study, we found that the oral administration of PL201A, a designed analog of phenylpropanoids, which are a family of natural products with antiaging effects, promoted the neurogenesis and proliferation of NPCs and ameliorated cognitive impairment in a transgenic mouse model of AD. Furthermore, PL201A attenuated amyloid-β–induced mitochondrial stress and promoted NPC proliferation in vitro. Further mechanistic studies showed that PL201A restored the activation of AMP-regulated protein kinase–retinoblastoma signaling, which was suppressed by amyloid-β. Our findings suggest that PL201A may represent a promising regenerative therapeutic agent for cognitive decline in neurodegenerative diseases.

1. Introduction

Alzheimer's disease (AD) is a progressive neurodegenerative disorder that is characterized by deteriorating memory (Shabestari et al., 2016). The formation of amyloid-β (Aβ) plaques and neurofibrillary tangles containing the tau protein as well as neuronal and synaptic loss, are the main pathological characteristics of AD (Das et al., 2014; DeToma et al., 2014).

In the adult mammalian brain, neurogenesis occurs throughout life to maintain neural networks. In hippocampus, neurogenesis starts with generating neural progenitor cells (NPCs) from $Nestin^{+}SOX2^{+}GFAP^{+}$ radial glia-like cells in the subgranule zone in dentate gyrus. After several rounds of proliferation, these NPCs become neuroblasts and further develop into immature neurons expressing doublecortin, which subsequently migrate into the granular cell layer and give rise to NEUN-positive mature dentate granule neurons (Goncalves et al., 2016). Evidence has demonstrated that adult hippocampal NPC proliferation and neurogenesis are dysregulated in AD patients and animal models, contributing to cognitive decline in AD (Boekhoorn et al., 2006; Crews et al., 2010; Feng et al., 2001; Li et al., 2008). Therefore, restoring endogenous

* Corresponding author at: State Key Laboratory of Bioorganic and Natural Products Chemistry, Center for Excellence in Molecular Synthesis, Shanghai Institute of Organic Chemistry, Chinese Academy of Sciences, 345 Lingling Road, Shanghai, 200032, China. Tel.: +86-21-54925131.
** Corresponding author at: State Key Laboratory of Cell Biology, Institute of Biochemistry and Cell Biology, Shanghai Institutes for Biological Sciences, Chinese Academy of Sciences, 320 Yueyang Road, Shanghai 200031, China. Tel./fax: 86-21-54921374.
E-mail addresses: byu@sioc.ac.cn (B. Yu), gpei@sibs.ac.cn (G. Pei).
[1] Co-first author.

0197-4580/$ – see front matter © 2019 Elsevier Inc. All rights reserved.
https://doi.org/10.1016/j.neurobiolaging.2019.05.002

NPC proliferation and neurogenesis may provide a promising therapeutic target for AD treatment.

Mitochondria play a central role in energy metabolism by producing adenosine triphosphate (ATP) via the electron transport chain and oxidative phosphorylation and are critically involved in the process of neurogenesis (Beckervordersandforth et al., 2017; Khacho and Slack, 2018; Schon and Przedborski, 2011). Mounting evidence has shown that mitochondrial function is impaired during AD pathogenesis in patients and transgenic mouse models (Hirai et al., 2001; Manczak et al., 2011; Pedros et al., 2014). Furthermore, Aβ has been found to be localized in mitochondria and to impair mitochondrial dynamics and bioenergetics (Chiang et al., 2016; Cho et al., 2009; Lustbader et al., 2004; Pagani and Eckert, 2011; Wang et al., 2008, 2009). Moreover, given that restoring mitochondrial function with pharmacological agents ameliorates age-related neurogenesis defects and cognitive impairments, it is possible that such mitochondrial-affecting agents can promote neurogenesis and alleviate AD pathogenesis (Beckervordersandforth et al., 2017; Puri, 2017).

Natural products provide a rich resource for the discovery of new drug leads because of their unique structures and properties (Newman and Cragg, 2016). However, for several reasons, such as their low content in herbs, their application is limited; therefore, synthetic strategies are applied to overcome these problems. Phenylpropanoids, which are reported to exert antiaging effects, are a family of natural products synthesized by plants (Gao et al., 2015; Grond et al., 2000; Kim, 2010). As a widely studied phenylpropanoids, quercetin has been revealed to inhibit cell oxidation and inflammation and to minimize the progression of neurodegenerative diseases such as AD and PD (Kolaj et al., 2018). Coumarins are another important class of phenylpropanoids, and they have been reported to inhibit acetylcholinesterase activity and ameliorate AD progression (Anand et al., 2012). In this study, we reported that PL201A, a designed analog from phenylpropanoids, ameliorated cognitive impairments and enhanced NPC proliferation and neurogenesis in transgenic AD mice. Moreover, we found that PL201A attenuated Aβ-associated mitochondrial dysfunction and NPC proliferation defects in human NPCs. Further mechanistic studies revealed that Aβ-induced dysregulation of the AMP-activated protein kinase (AMPK) pathway is restored by PL201A. Collectively, our data suggest that PL201A can serve as a regenerative therapeutic agent for cognitive decline in neurodegenerative diseases.

2. Methods

2.1. Animals

APP/PS transgenic mice (Jackson Laboratory, stock number 004462) coexpress chimeric mouse/human APP containing the K595N/M596L Swedish mutations (APPswe) and mutant human PS1 with a deletion of exon 9 (PS1ΔE9) under the control of mouse prion promoter elements. These mice were maintained and genotyped according to the guidance provided by Jackson Laboratory. Gender- and age-matched wild-type (WT) littermates were used as controls. The experimental procedures for the use and care of the animals were approved by the Ethics Committee of the Shanghai Institutes for Biological Sciences, Chinese Academy of Sciences. All mice were given ad libitum access to food and water.

2.2. General synthesis methods

All reactions were carried out under nitrogen or argon with anhydrous solvents in flame-dried glassware, unless otherwise noted. The chemicals used were reagent grade as supplied, except where noted.

2.3. Synthesis of PL201A

Rhamnopyranosyl trichloroacetimidate (Angelika and Richerd, 1988; Larson and Heathcock, 1997) (430 mg, 0.1 mmol) and (4-*O*-*tert*-butyldimethylsilyl) ferulic acid (Fache et al., 2005) (310 mg, 0.1 mmol) were combined in a flask and concentrated from dry CH_2Cl_2. The resulting residue was dissolved in 2.0 mL of dry CH_2Cl_2, and 220 μL of 0.1 M TMSOTf in CH_2Cl_2 was added over 20 minutes. After the reaction mixture was stirred for an additional 30 minutes, 5 mL of saturated $NaHCO_3$ was added with vigorous stirring. After extraction with CH_2Cl_2, the combined organic layers were dried over $MgSO_4$ and concentrated. The residue was purified by chromatography on silica gel with eluent (petroleum ether-EtOAc, 5:1), and the α-L-rhamnopyranoside product (495 mg, 85%) was obtained. A solution of the α-L-rhamnopyranoside product (490 mg, 0.85 mmol) and tetrabutylammonium fluoride 1.7 mL (1 M solution in tetrahydrofuran) in dry tetrahydrofuran (2.0 mL) was stirred at room temperature for 2 hours and then diluted with ether. The organic layer was washed with brine, dried over $MgSO_4$, and concentrated in vacuo. The obtained residue was dissolved in methanol (2.0 mL) at 0 °C, then 33% CH_3NH_2 in methanol solution (3.0 mL) was added in 5 minutes and the reaction was stirred for 2 hours at 0 °C. The reaction was then evaporated under reduced pressure and purified by column chromatography (gradient EtOAc to EtOAc: MeOH = 10: 1), and PL201A (172 mg, 60%) was obtained. [α]D17= −39.6 (c 1.0, MeOH); ESI(+)-MS: 341.3 [M+1]+; 1H-NMR (CD3OD, 400 MHz) δ 7.62–7.66 (d, J = 16 Hz, 1H), 7.20 (s, 1H), 7.06–7.08 (d, J = 8 Hz, 1H), 6.78–6.80 (d, J = 8 Hz, 1H), 6.33–6.37 (d, J = 16 Hz, 1H), 6.02 (d, J = 1.2 Hz, 1H), 3.87 (s, 3H), 3.74–3.77 (dd, J1 = 3.6 Hz, J2 = 9.6 Hz, 1H), 3.68–3.72 (m, 1H), 3.43–3.47 (t, J1 = 9.6 Hz, J2 = 19.2 Hz, 1H), 3.28 (s, 1H), 1.25–1.26 (d, J = 6.4 Hz, 3H); 13C NMR (CD3OD, 126 MHz) δ 167.17, 151.07, 149.49, 148.14, 127.63, 124.55, 116.67, 114.87, 111.92, 95.47, 73.70, 72.44, 72.32, 71.50, 56.67, 18.24. A flowchart summarizing the synthesis of PL201A is provided in Fig. S1.

2.4. Drug administration and BrdU injections

PL201A was dissolved in water. APP/PS or WT mice were orally administered 10 mg/kg PL201A or vehicle (water) once per day for 90 days. To assess the effects of PL201A on neurogenesis, mice received intraperitoneal injection of BrdU (50 mg/kg) once per day from day 74 to day 80 of drug administration. After the end of Morris water maze (MWM) testing on day 102, the animals were transcardially perfused successively with cold PBS and 4% paraformaldehyde (PFA).

2.5. Morris water maze test

MWM testing was performed as previously described with modifications (Morris, 1984; Teng et al., 2010). The apparatus consisted of a 120-cm diameter circular pool filled with water and small white plastic balls and maintained at 22.0 ± 0.5 °C. A transparent 11-cm diameter platform was placed 1 cm below the water surface at a fixed point in one quadrant. Approximately equal numbers of male and female mice were included in each experimental group. The animals were brought into the behavior room, acclimatized and trained. The training protocol consisted of 6 consecutive days with four trials per day. On day 4 and 24 hours after the last training trial, a probe trial was conducted. The swimming paths were monitored using an automated tracking system (Ethovision XT software).

2.6. Cell culture and EdU incorporation assay

Human iPSC-derived NPCs were provided by IxCell Biotechnology Co, Ltd, and a monolayer cell culture was maintained in B27- and N2-supplemented DMEM/F12 and neurobasal medium (1:1) with 10 ng/mL bFGF, 10 ng/mL leukemia inhibitory factor, 3 μM CHIR99021, 5 μM SB431542, and 200 μM ascorbic acid in Matrigel (Corning)–coated dishes. For the EdU incorporation assay, the cells were dissociated with Accutase (Sigma Aldrich) and seeded at a density of 1.5 x10^4 cells/cm^2 in poly-D-lysine and laminin-coated 96-well plates in B27- and N2-supplemented DMEM/F12 and neurobasal medium (1:1) containing 10 ng/mL bFGF. On the following day, the cells were pretreated with or without Aβ (5 μM; GenicBio), oligomycin (1 μM; Selleck) and compound C (10 μM; Selleck) for 30 minutes before 30 μM PL201A was added. The cells were incubated for 72 hours and EdU (10 μM; Sigma Aldrich) was added 30 minutes before fixation. Afterward, the NPCs were fixed in 4% PFA for 15 minutes and permeabilized with 0.1% Triton X-100 in PBS. EdU staining was performed according to the manufacturer's protocol (Click-iT, Invitrogen). Cellomics ArrayScan VTI 700 (Thermo Scientific) was used to scan and analyze the stained cells. To prepare the Aβ1–42 oligomer, Aβ1–42 peptide (GenicBio) was added to hexafluoroisopropanol, and the mixture was air-dried and vacuum concentrated to form a film. Then, it was dissolved in dimethylsulfoxide at a concentration of 5 mM and further diluted with PBS to 100 μM. The solution was incubated at 4 °C for 24 hours to promote peptide self-aggregation.

2.7. Western blotting

Human iPSC-derived NPCs were seeded at a density of 1.2×10^5 cells/well in B27- and N2-supplemented DMEM/F12 and neurobasal medium (1:1) with 10 ng/mL bFGF. On the following day, the cells were pretreated with 5 μM Aβ for 30 minutes. Then 30 μM PL201A was added and the cells were further incubated for 72 hours. After that, the cells were washed with cold PBS and lysed with Laemmli sample buffer. The cell lysates were resolved by SDS/PAGE and transferred to a nitrocellulose membrane. The following rabbit monoclonal antibodies were used: anti–phospho-AMPK (Tyr172, 1:1000, Beyotime), anti–phospho-Rb (Ser807/811, 1:1000, Beyotime), anti-AMPK (1:500, Beyotime), and anti-Rb (1:400, BOSTER). The blots were analyzed by the chemiluminescent detection (BioRad) of a peroxidase-conjugated, subtype-specific antibody (1:5000, Abmart).

2.8. Tissue preparation and immunohistochemistry

For immunohistochemistry, the animals were anesthetized and transcardially perfused with 4% PFA. The brains were dissected, postfixed with 4% PFA for 24 hours and stored in a 30% sucrose solution for 72 hours. Coronal sections were collected as 30-μm free-floating cryosections. For BrdU staining, the sections were treated with 2 M HCl at 37 °C for 20 minutes and rinsed in 0.1 M borate buffer (pH 8.5). For NEUN, SOX2, and KI67 staining, antigen retrieval was performed with citrate buffer (10 mM, pH 6.5) for 20 minutes at 95 °C. After that, the sections were blocked with 3% donkey serum and 0.3% Triton-X. These samples were then incubated in primary and secondary antibodies at 4 °C overnight and at RT for 1 hour. The samples were imaged with an Olympus FV100i confocal microscope and analyzed with Image-Pro Plus software. The antibodies were diluted as follows: rat anti-BrdU antibody (1:2000; AbD Serotec), rabbit anti-NEUN (1:200; Millipore), rabbit anti-KI67 (1:100; Abcam), and goat anti-SOX2 (1:100; R&D Systems).

For quantitative analysis, every ninth section through the entire DG was processed. For each section, a stack of approximately 12–13 overlapping images were captured with a 2 μm step from the top to the bottom layer. All of the stained cells within the subgranular zone or the granular cell layer were counted, and the cell densities were evaluated by dividing the number of cells by the area and 30-μm of thickness. The colocalization of staining for the different antibodies was confirmed in three dimensions in the double-stained cells. All quantification was performed in a double-blinded manner.

2.9. ATP assay

Cellular ATP levels were measured with the CellTiter-Glo Luminescent Assay (Promega) according to the manufacturer's protocol. Cell counts were determined by Hoechst 33342 staining.

2.10. Mitochondrial morphology analysis

Mitochondrial morphology was assessed by staining with MitoTracker Green (Beyotime) according to the manufacturer's protocol. Briefly, NPCs were stained with 50 nM MitoTracker Green at 37 °C for 45 minutes. Then, the cells were imaged with an Olympus FV1200 confocal microscope. Quantification was performed with ImageJ using a macro developed by Ruben K. Dagda (Dagda et al., 2009). Briefly, the area of interest (one cell) was selected with the polygon selection tool. Then, the image was sharpened and automatically thresholded. Next, different mitochondrial parameters, including the mitochondrial area and aspect ratio (major/minor axis) were obtained using the analyze particles tool. All quantification was performed in a double-blinded manner.

2.11. Mitochondrial membrane potential quantification

The mitochondrial membrane potential was assessed with JC-1 (Beyotime) according to the manufacturer's protocol. Generally, monolayer NPC cultures were pretreated with Aβ for 30 minutes in culture medium containing 10 ng/mL bFGF. Then 30 μM PL201A was added and the cell were further incubated for 72 hours. After Aβ and PL201A treatment, the NPCs were incubated with JC-1 for 20 minutes in staining buffer solution at 37 °C. The fluorescence intensity was determined by an Olympus FV100i microscope and analyzed with ImageJ software (green fluorescence: 530 nm, red fluorescence: 590 nm). The same exposure time and laser intensities were applied during all acquisitions. The membrane potential was represented as the ratio of red/green fluorescence intensity. All quantification was performed in a double-blinded manner.

2.12. Detection of mitochondrial reactive oxygen species

Mitochondrial reactive oxygen species (ROS) production was detected using MitoSOX Red Mitochondrial Superoxide Indicator (Thermo Fisher) following the manufacturer's protocol. Briefly, NPCs were incubated with 5 μM MitoSOX for 10 minutes at 37 °C. After three washes with PBS, images of the cells were taken using a Zeiss Observer Z1 microscope. The same exposure time and laser intensities were applied during all acquisitions. Fluorescence intensity was assessed by ImageJ software and normalized to cell number, which was measured using Hoechst 33342 staining. All quantification was performed in a double-blinded manner.

2.13. Statistical analysis

All quantified data are presented as the mean ± SEM. The results were analyzed by a two-tailed *t* test to determine the statistical

significance of the treatment sets. For multiple comparisons, the results were analyzed by one-way analysis of variance (ANOVA) or two-way ANOVA followed by Bonferroni test when appropriate with GraphPad Prism 6 Software. If the normality tests failed, a Kruskal-Wallis test on ranks followed by a Dunn's posttest was performed. *p*-values less than 0.05 ($p < 0.05$) were considered indicative of significance.

3. Results

3.1. PL201A ameliorates cognitive deficits in a mouse model of Alzheimer's disease

To evaluate the effects of PL201A (Fig. 1A) on the pathophysiology of AD, two groups of 5-month-old APP/PS1 mice were

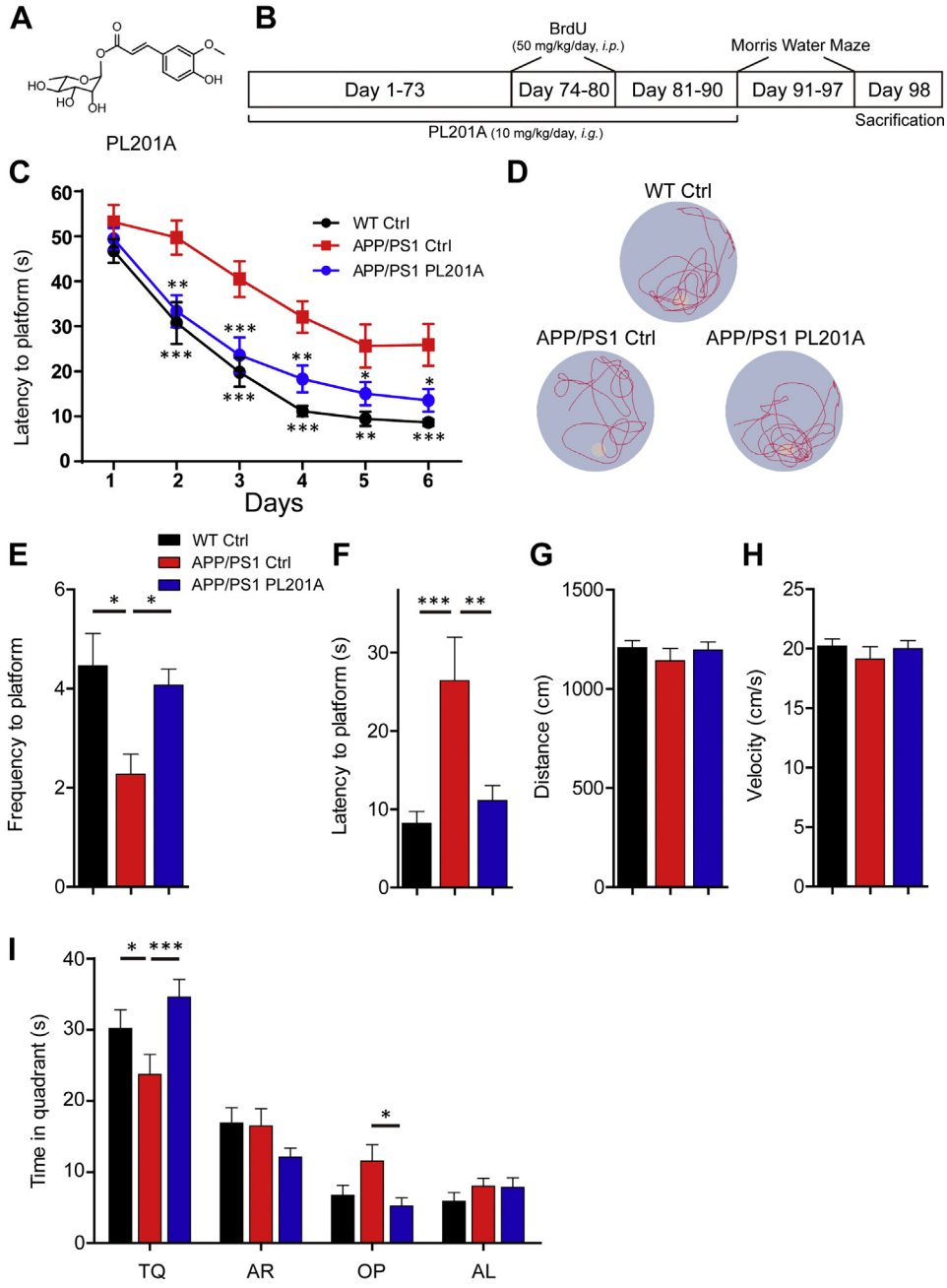

Fig. 1. The administration of PL201A ameliorates cognitive impairments in transgenic AD mice. (A) The structure of PL201A. (B) The experimental schedule for neurogenesis analysis and Morris water maze (MWM) testing. (C) The learning curves of the mice from the different treatment groups over the various training days (n = 11–14 per group). (D) Representative tracks of the mice in the probe trial on day 7 are shown. (E and F) The frequency with which the target position was passed (D) and the latency to find the platform (E) in the probe trial on day 7 (n = 11–14 per group). (G and H) The swimming distance (F) and velocity (G) of the mice in the probe trial on day 7 (n = 11–14 per group). (I) The comparison of the time spent in the target quadrant in the probe trial on day 7 (n = 11–14 per group). The data are presented as the mean ± SEM; $^{*}p < 0.05$, $^{**}p < 0.01$, $^{***}p < 0.001$, analyzed by two-way ANOVA test followed by Bonferroni (C, I), by one-way ANOVA followed by Bonferroni test (F) or by Kruskal-Wallis test on ranks followed by a Dunn's posttest when the test for normality failed (Kolmogorov-Smirnov test) (E, G, H). Abbreviations: AD, Alzheimer's disease; ANOVA, analysis of variance; TQ, target quadrant; AR, adjacent right; OP, opposite; AL, adjacent left.

gavaged daily with PL201A (10 mg/kg/d) or vehicle for 90 days. Thereafter, spatial memory was assessed using the MWM (Fig. 1B). Two-way ANOVA was performed to analyze the latency to platform and a significant difference was observed among groups [$F(2,210)=42.991$, $p < 0.001$]. Compared with their WT littermates, the APP/PS1 mice exhibited a significantly slower learning rate, indicating cognitive deficits in these mice [day 4, $t(22)=6.335$, $p < 0.001$]. Notably, chronic PL201A treatment significantly [day 4, $t(23)=3.143$, $p = 0.0046$] ameliorated learning and memory impairment in the APP/PS1 mice (Fig. 1C). To assess reference memory, a probe trial was administered on day 7. Compared with the vehicle-treated mice, the PL201A-treated APP/PS1 mice crossed the platform area more often (Fig. 1D and E, $p = 0.0264$), took less time to reach the position of platform (Fig. 1F, $p = 0.0035$), and spent more time in the target quadrant (Fig. 1I, $p < 0.001$). There was no detectable difference in swimming distance or velocity between the vehicle- and PL201A-treated mice, suggesting that PL201A had little influence on the motor ability or motivation of these mice (Fig. 1G and H). Together, our data indicate that the administration of PL201A ameliorates cognitive deficits in transgenic AD model mice.

3.2. PL201A promotes neurogenesis and NPC proliferation in a mouse model of Alzheimer's disease

The disease-related decline in hippocampal neurogenesis is linked to cognitive impairment in AD. To examine the effects of PL201A on hippocampal neurogenesis, PL201 or vehicle-treated APP/PS1 mice received BrdU injections once a day for 7 consecutive days and the mice were sacrificed 28 days after the first injection (Fig. 1A). Then the numbers of newly generated NEUN/BrdU -double-positive cells in the hippocampus was analyzed. Compared with the vehicle-treated group, the PL201A-treated mice exhibited a significantly increased numbers of $NEUN^+/BrdU^+$ cells (Fig. 2A–C). In addition, there was no difference in the percentage of BrdU-positive cells that were $NEUN^+/BrdU^+$ between the vehicle and PL201A-treated groups (Fig. 2D), indicating that PL201A may promote neurogenesis by enhancing NPC proliferation instead of altering neuronal lineage commitment. Afterward, the proliferation of NPCs in the subgranule zone was examined. The quantification showed that there were more KI67+/SOX2+ proliferating NPCs in the PL201-treated APP/PS1 mice (Fig. 2E–G). Taken together, these data indicate that PL201A can promote neurogenesis and NPC proliferation in transgenic AD model mice. In addition, compared with the vehicle-treated group, we observed the number of GFAP+ cells was slightly reduced (about 15%, data not shown) after PL201A treatment, suggesting PL201A may modulate neuroinflammation.

3.3. PL201A attenuates Aβ-induced mitochondrial stress in human NPCs

Because mitochondrial function has been shown to play a key role in the proliferative potential of stem cells (Rafalski and Brunet, 2011), we wondered whether PL201A modulates mitochondrial functions to exert its effects on NPCs. To answer this question, the mitochondrial membrane potential and cellular ATP levels of human NPCs were evaluated after incubation with a 5 μM Aβ1–42 oligomer-containing preparation or 30 μM PL201A. We found that incubation with Aβ1–42 reduced the mitochondrial membrane potential and cellular ATP levels of NPCs, which were partially resorted by PL201A treatment (Fig. 3A–C). Evidence from cellular and animal models of AD has shown that Aβ1–42 elevates the production of ROS and leads to cytotoxicity. MitoSOX fluorescence staining revealed that mitochondrial ROS levels increased after 5 μM Aβ1–42 treatment, whereas cotreatment with 30 μM PL201A abolished this Aβ-induced effect (Fig. 3D). To further assess whether mitochondrial morphology and dynamics are also modulated by PL201A, we labeled mitochondria with MitoTracker Green and observed that NPCs exposed to Aβ1–42 exhibited decreased mitochondrial area and aspect ratio, and these effects were attenuated on PL201A treatment (Fig. 3E–G). In addition, Aβ1–42 inhibited the expression of the mitochondrial fusion mediator *MFN1*, and this was also partially rescued by PL201A (Fig. 3H). We

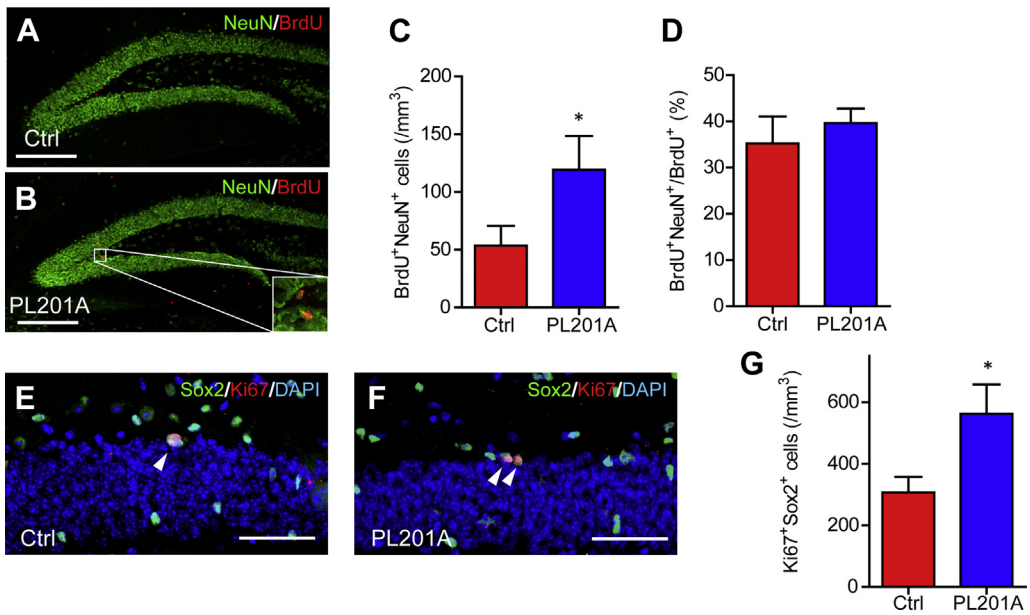

Fig. 2. Neurogenesis and NPC proliferation is enhanced by PL201A in transgenic AD mice. (A and B) Confocal photomicrographs of NEUN and BrdU immunostaining in the dentate gyrus (DG) of the mice treated with vehicle (A) and PL201A (B). Scale bars, 200 μm. (C) The quantification of $NEUN^+BrdU^+$ cells in the DG of the mice in (A) and (B) (n = 6–8 per group). (D) The proportion of $BrdU^+$ cells that were $BrdU^+NEUN^+$. (E and F) Representative images of SOX2, KI67, and DAPI immunostaining of the dentate gyrus (DG) of the mice treated with vehicle (E) and PL201A (F). Scale bars, 50 μm. (G) The quantification of $KI67^+SOX2^+$ cells in the DG of the mice in (E) and (F) (n = 6 per group). The data are presented as the mean ± SEM. $^*p < 0.05$, analyzed by a two-tailed *t* test. Abbreviations: AD, Alzheimer's disease.

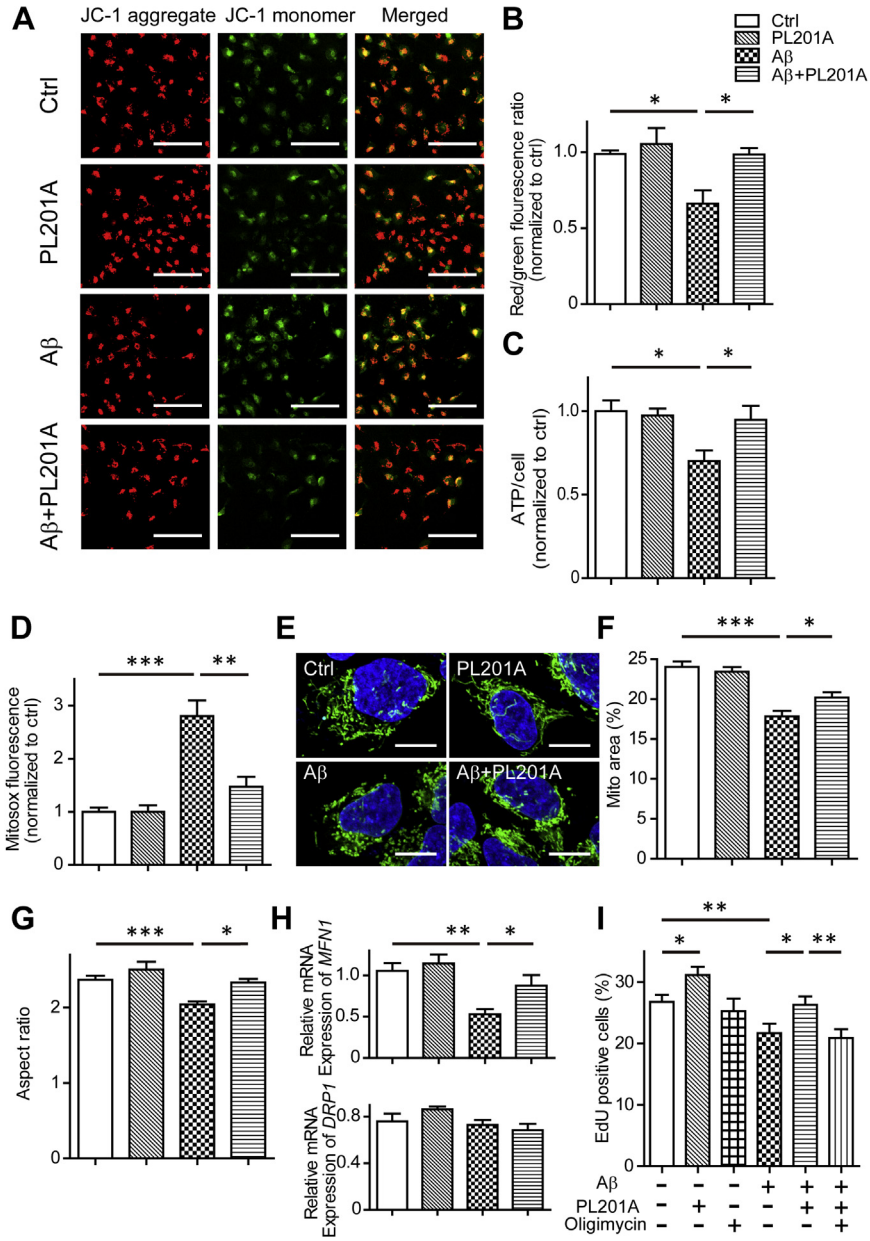

Fig. 3. PL201A attenuates amyloid-β-associated mitochondrial stress. (A) The mitochondrial membrane potential of NPCs was evaluated by JC-1 staining and representative fluorescence images are shown. Scale bars, 100 μm. (B) The quantification of the mitochondrial membrane potential of NPCs in (A), which is demonstrated by the ratio of red (JC-1 aggregates) to green (JC-1 monomers) fluorescence intensity. n = 5 independent experiments. (C) ATP in the cells subjected to the same conditions as in (A). n = 3 independent experiments. (D) MitoSOX fluorescence in the cells subjected to the same conditions as in (A). n = 3 independent experiments. (E) Representative confocal images of the mitochondrial morphology of NPCs treated as in A. Scale bars, 10 μm. (F and G) The analysis of the mitochondrial area and aspect ratio (long/short axis) as in D. The experiment was performed three times with 35–46 images per treatment group. (H) Gene expression analysis of *MFN1* and *DRP1*. n = 5 independent experiments. (I) The proliferation of NPC was evaluated by EdU staining. n = 13 independent experiments. The data are presented as the mean ± SEM. $^{*}p < 0.05$, $^{**}p < 0.01$, $^{***}p < 0.001$, analyzed by one-way ANOVA test followed by Fisher's protected least significant difference test. Abbreviations: ANOVA, analysis of variance; NPC, neural progenitor cell. (For interpretation of the references to color in this figure legend, the reader is referred to the Web version of this article.)

next investigated whether the enhancement of NPC proliferation on PL201A treatment is associated with the mitochondrial modulating effect of PL201A. An EdU incorporation assay was performed to examine the effects of Aβ1–42 and PL201A on NPC proliferation. Compared with vehicle-treated cells, the cells treated with 30 μM PL201A alone exhibited an enhanced ratio of EdU^{+} cells. In addition, 5 μM Aβ1–42 treatment significantly reduced EdU incorporation, whereas cotreatment with 30 μM PL201A resulted in a weakening of this reduction. Moreover, when 1 μM oligomycin, a mitochondrial inhibitor, was added to NPC cultures treated with Aβ1–42 and PL201A, the PL201A-mediated restoration in EdU incorporation was abolished (Fig. 3I). These results indicate that PL201 regulates mitochondrial functions to enhance NPC proliferation.

3.4. PL201A alleviates the Aβ-associated dysregulation of AMPK signaling

AMPK plays a central role in mitochondrial metabolism and is a crucial regulator of energy homeostasis. On exposure to a 5 μM Aβ1–42 oligomer-containing preparation, AMPK phosphorylation

was markedly suppressed in the NPCs, indicating disrupted cellular metabolism. Cotreatment with 30 μM PL201A attenuated the Aβ1–42-induced decrease in AMPK activation (Fig. 4A and B). Because it has been reported that AMPK directly phosphorylates Rb to promote NPC proliferation (Dasgupta and Milbrandt, 2009), Rb phosphorylation levels were also analyzed on Aβ and PL201A treatment, and similar results were observed (Fig. 4C and D). Moreover, blocking AMPK activation with compound C partially abolished the PL201A-restored NPC proliferation (Fig. 4E). Together, these results indicate that PL201A may counteract the Aβ1–42-induced decline in NPC proliferation by reversing mitochondrial dysfunction and activating AMPK-Rb signaling (Fig. 4F).

4. Discussion

Alzheimer's disease is an incurable degenerative disease that is common in the elderly population. A number of pharmacological agents have been investigated for treating AD, and natural products are important sources of new drug leads because of their wide chemical diversity. In this study, we showed that PL201A, a designed analog from natural products, ameliorates cognitive impairment and enhances neurogenesis and NPC proliferation in transgenic AD mice, suggesting that PL201A may serve as a regenerative therapeutic agent for cognitive decline in neurodegenerative diseases.

Accumulating evidence suggests that mitochondrial dysfunction is deeply involved in the onset and progression of AD (Lin and Beal, 2006; Wang et al., 2007). Improving mitochondrial functions has been reported to protect neurons from Aβ toxicity and restore synaptic function (Du et al., 2008). Moreover, it has been also reported that mitochondrial impairment is induced by inflammatory mediators including oxidative stress and proinflammatory cytokines, whereas mitochondrial dysfunction conversely exacerbates microglia-mediated neuroinflammation (Di Filippo et al., 2010; Onyango et al., 2016; Wilkins and Swerdlow, 2016). NPC proliferation and neurogenesis are important for neuroprotection in aging and neurodegenerative diseases such as AD. It has been reported that mitochondrial fusion and decreased ROS levels facilitate the self-renewal of neural stem cells (Khacho et al., 2016). In line with this study, we found that PL201A inhibits the Aβ-induced fragmentation of mitochondria and elevation of ROS levels, suggesting that modulating mitochondria dynamics and ROS levels may be a potential strategy for neuroprotection in AD. These reports, together with our findings that PL201A attenuates Aβ-associated mitochondrial dysfunction and promotes NPC proliferation, indicate that mitochondria-targeted intervention is beneficial for

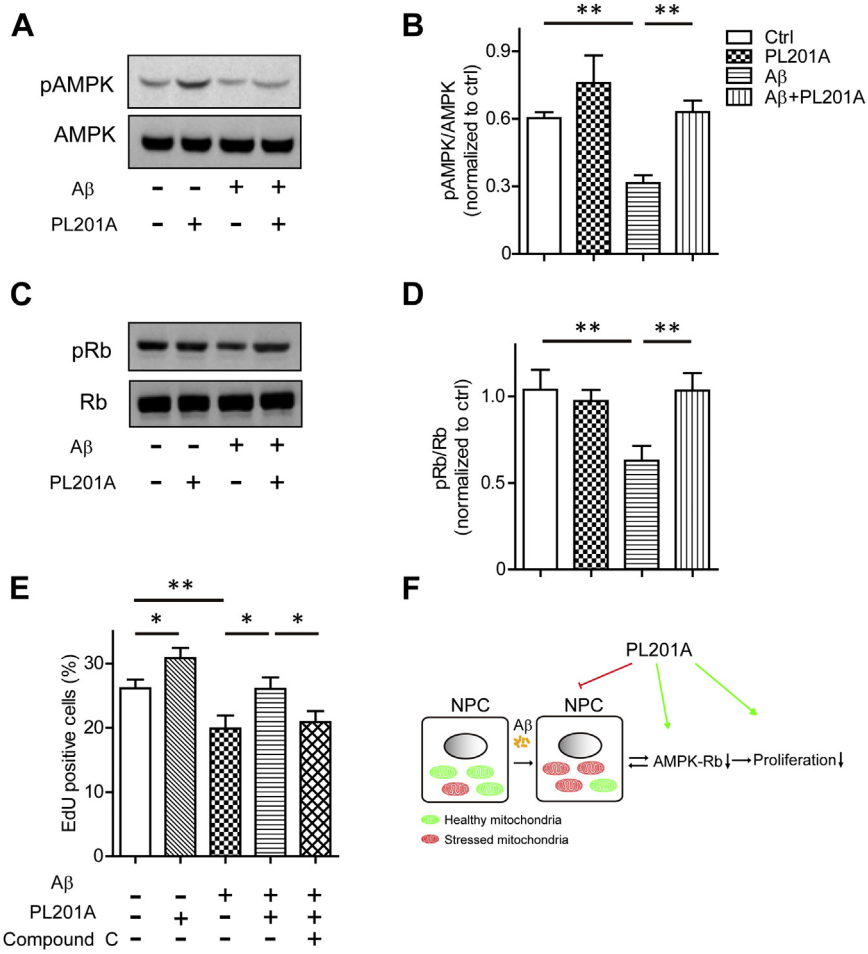

Fig. 4. Amyloid-β-induced dysregulation of AMPK is alleviated by PL201A. (A and B) AMPK activation was analyzed by western blotting with antibodies against the phosphorylated and total AMPK. n = 6 independent experiments. (C and D) Cells were treated as in (A) and Rb phosphorylation was analyzed by western blotting with antibodies against the phosphorylated and total AMPK. n = 6 independent experiments. (E) The proliferation of NPC was evaluated by EdU staining. n = 9 independent experiments. (F) A schematic diagram showing that PL201A counteracts Aβ1–42-induced decline in NPC proliferation by improving mitochondrial dysfunction and activating AMPK-Rb signaling. The data are presented as the mean ± SEM. $^{*}p < 0.05$, $^{**}p < 0.01$, analyzed by one-way ANOVA test followed by Fisher's protected least significant difference test. Abbreviations: ANOVA, analysis of variance; NPC, neural progenitor cell.

restoring multiple cellular functions that are impaired in AD pathogenesis, and suggest that mitochondria may be a promising target for developing anti-AD therapies.

Metabolic signaling pathways have pivotal roles in modulating NPC activity (Knobloch et al., 2013). Consistent with previous findings in other cell types (Lin et al., 2016), our study revealed that Aβ reduces AMPK activation and NPC proliferation and that these effects are alleviated by PL201A treatment. In addition to data that suggests that AMPK promotes neurogenesis, emerging evidence has also revealed that AMPK is involved in the pathogenesis of AD through regulating amyloidogenesis and tau protein phosphorylation (Cai et al., 2012; Won et al., 2010). In addition, AMPK has been reported to activate autophagy by targeting autophagy proteins such as ULK1, thereby influencing the metabolism of the Aβ and tau proteins (Anand et al., 2012; Kolaj et al., 2018). In the present study, we observed that PL201A treatment increased mitochondrial mass. Based on the fact that PGC-1α, which is critical for mitochondrial biogenesis and autophagy, is another important downstream target of AMPK, it is possible that PL201A also promotes PGC-1α synthesis (Herzig and Shaw, 2018). Taken together, these findings indicate that AMPK-modulating agents such as PL201A may exert multiple anti-AD effects. Although it is often assumed that an increased AMP/ATP ratio activates AMPK, we observed in our study that Aβ decreased AMPK activation while reducing ATP production. Because AMP/ATP-independent AMPK regulation has been reported, it is possible that a similar mechanism may contribute to the effect of Aβ on AMPK as well (Racioppi and Means, 2012; Zhang et al., 2017). Our results not only provide evidence for the regulatory role of AMPK in Aβ-associated deficits in NPC proliferation but also present PL201A as a potential therapeutic treatment for AD.

Disclosure

The authors declare no conflict of interest.

Acknowledgements

The authors are grateful to Jing Lu, Qinying Wang, and Jianxin Mao for technical assistance and helpful discussion. They thank all members of the laboratory for sharing reagents and advice. Their work using Cellomics ArrayScan VTI 700 was performed at the National Center for Protein Science Shanghai. This work was supported by the “Organ Reconstruction and Manufacturing”, Strategic Priority Research Program of the Chinese Academy of Sciences [XDA16000000, XDA16010309], the Program of the International Science & Technology Cooperation Program of China (2016YFE0103500), and the National Key Research and Development Program of China [2018YFA0108000, 2018YFA0108003].

Authors’ contributions: GP and BY conceived the project and revised the manuscript; S-CH designed the experiments and drafted the manuscript. XC designed and established the compound library and contributed to writing the manuscript. S-CH, XC, YZ, F-CS, S-MX, Y-QA, L-FG, Y-FY, and S-FH carried out the experiments and analyzed the data.

Appendix A. Supplementary data

Supplementary data to this article can be found online at https://doi.org/10.1016/j.neurobiolaging.2019.05.002.

References

Anand, P., Singh, B., Singh, N., 2012. A review on coumarins as acetylcholinesterase inhibitors for Alzheimer's disease. Bioorg. Med. Chem. 20, 1175–1180.

Angelika, E.W., Richard, S.R., 1988. Glycosyl imidates, 37. Direct O-glycosylation of compounds containing a PO(OH) moiety. Liebigs Ann. Chem. 1988, 675–678.

Beckervordersandforth, R., Ebert, B., Schaffner, I., Moss, J., Fiebig, C., Shin, J., Moore, D.L., Ghosh, L., Trinchero, M.F., Stockburger, C., Friedland, K., Steib, K., von Wittgenstein, J., Keiner, S., Redecker, C., Holter, S.M., Xiang, W., Wurst, W., Jagasia, R., Schinder, A.F., Ming, G.L., Toni, N., Jessberger, S., Song, H., Lie, D.C., 2017. Role of mitochondrial metabolism in the control of early lineage progression and aging phenotypes in adult hippocampal neurogenesis. Neuron 93, 560–573.e566.

Boekhoorn, K., Joels, M., Lucassen, P.J., 2006. Increased proliferation reflects glial and vascular-associated changes, but not neurogenesis in the presenile Alzheimer hippocampus. Neurobiol. Dis. 24, 1–14.

Cai, Z., Yan, L.J., Li, K., Quazi, S.H., Zhao, B., 2012. Roles of AMP-activated protein kinase in Alzheimer's disease. Neuromolecular Med. 14, 1–14.

Chiang, M.C., Nicol, C.J., Cheng, Y.C., Lin, K.H., Yen, C.H., Lin, C.H., 2016. Rosiglitazone activation of PPARgamma-dependent pathways is neuroprotective in human neural stem cells against amyloid-beta-induced mitochondrial dysfunction and oxidative stress. Neurobiol. Aging 40, 181–190.

Cho, D.H., Nakamura, T., Fang, J., Cieplak, P., Godzik, A., Gu, Z., Lipton, S.A., 2009. S-nitrosylation of Drp1 mediates beta-amyloid-related mitochondrial fission and neuronal injury. Science 324, 102–105.

Crews, L., Adame, A., Patrick, C., Delaney, A., Pham, E., Rockenstein, E., Hansen, L., Masliah, E., 2010. Increased BMP6 levels in the brains of Alzheimer's disease patients and APP transgenic mice are accompanied by impaired neurogenesis. J. Neurosci. 30, 12252–12262.

Dagda, R.K., Cherra 3rd, S.J., Kulich, S.M., Tandon, A., Park, D., Chu, C.T., 2009. Loss of PINK1 function promotes mitophagy through effects on oxidative stress and mitochondrial fission. J. Biol. Chem. 284, 13843–13855.

Das, P., Kang, S.G., Temple, S., Belfort, G., 2014. Interaction of amyloid inhibitor proteins with amyloid beta peptides: insight from molecular dynamics simulations. PLoS One 9, e113041.

Dasgupta, B., Milbrandt, J., 2009. AMP-activated protein kinase phosphorylates retinoblastoma protein to control mammalian brain development. Dev. Cell. 16, 256–270.

DeToma, A.S., Krishnamoorthy, J., Nam, Y., Lee, H.J., Brender, J.R., Kochi, A., Lee, D., Onnis, V., Congiu, C., Manfredini, S., Vertuani, S., Balboni, G., Ramamoorthy, A., Lim, M.H., 2014. Synthetic flavonoids, aminoisoflavones: interaction and reactivity with metal-free and metal-associated amyloid-beta species. Chem. Sci. 5, 4851–4862.

Di Filippo, M., Chiasserini, D., Tozzi, A., Picconi, B., Calabresi, P., 2010. Mitochondria and the link between neuroinflammation and neurodegeneration. J. Alzheimers Dis. 20 (Suppl 2), S369–S379.

Du, H., Guo, L., Fang, F., Chen, D., Sosunov, A.A., McKhann, G.M., Yan, Y., Wang, C., Zhang, H., Molkentin, J.D., Gunn-Moore, F.J., Vonsattel, J.P., Arancio, O., Chen, J.X., Yan, S.D., 2008. Cyclophilin D deficiency attenuates mitochondrial and neuronal perturbation and ameliorates learning and memory in Alzheimer's disease. Nat. Med. 14, 1097–1105.

Fache, F., Suzan, N., Piva, O., 2005. Total synthesis of cimiracemate B and analogs. Tetrahedron 61, 5261–5266.

Feng, R., Rampon, C., Tang, Y.P., Shrom, D., Jin, J., Kyin, M., Sopher, B., Miller, M.W., Ware, C.B., Martin, G.M., Kim, S.H., Langdon, R.B., Sisodia, S.S., Tsien, J.Z., 2001. Deficient neurogenesis in forebrain-specific presenilin-1 knockout mice is associated with reduced clearance of hippocampal memory traces. Neuron 32, 911–926.

Gao, L., Peng, X.M., Huo, S.X., Liu, X.M., Yan, M., 2015. Memory enhancement of acteoside (verbascoside) in a senescent mice model induced by a combination of D-gal and AlCl3. Phytother. Res. 29 (8), 1131–1136.

Goncalves, J.T., Schafer, S.T., Gage, F.H., 2016. Adult neurogenesis in the hippocampus: from stem cells to behavior. Cell 167, 897–914.

Grond, S., Papastavrou, I., Zeeck, A., 2000. Structural diversity of 1-O-Acyl <alpha>-L-Rhamnopyranosides by precursor-directed biosynthesis with streptomyces griseoviridis. Eur. J. Org. Chem. 2000, 1875–1881.

Herzig, S., Shaw, R.J., 2018. AMPK: guardian of metabolism and mitochondrial homeostasis. Nat. Rev. Mol. Cell. Biol. 19, 121–135.

Hirai, K., Aliev, G., Nunomura, A., Fujioka, H., Russell, R.L., Atwood, C.S., Johnson, A.B., Kress, Y., Vinters, H.V., Tabaton, M., Shimohama, S., Cash, A.D., Siedlak, S.L., Harris, P.L., Jones, P.K., Petersen, R.B., Perry, G., Smith, M.A., 2001. Mitochondrial abnormalities in Alzheimer's disease. J. Neurosci. 21, 3017–3023.

Khacho, M., Slack, R.S., 2018. Mitochondrial dynamics in the regulation of neurogenesis: from development to the adult brain. Dev. Dyn. 247, 47–53.

Khacho, M., Clark, A., Svoboda, D.S., Azzi, J., MacLaurin, J.G., Meghaizel, C., Sesaki, H., Lagace, D.C., Germain, M., Harper, M.E., Park, D.S., Slack, R.S., 2016. Mitochondrial dynamics impacts stem cell identity and fate decisions by regulating a nuclear transcriptional program. Cell. Stem Cell. 19, 232–247.

Kim, Y.C., 2010. Neuroprotective phenolics in medicinal plants. Arch. Pharm. Res. 33, 1611–1632.

Knobloch, M., Braun, S.M., Zurkirchen, L., von Schoultz, C., Zamboni, N., Arauzo-Bravo, M.J., Kovacs, W.J., Karalay, O., Suter, U., Machado, R.A., Roccio, M., Lutolf, M.P., Semenkovich, C.F., Jessberger, S., 2013. Metabolic control of adult neural stem cell activity by fasn-dependent lipogenesis. Nature 493, 226–230.

Kolaj, I., Imindu Liyanage, S., Weaver, D.F., 2018. Phenylpropanoids and Alzheimer's disease: a potential therapeutic platform. Neurochem. Int. 120, 99–111.

Larson, D.P., Heathcock, C.H., 1997. Total synthesis of tricolorin A. J. Org. Chem. 62, 8406–8418.

Li, B., Yamamori, H., Tatebayashi, Y., Shafit-Zagardo, B., Tanimukai, H., Chen, S., Iqbal, K., Grundke-Iqbal, I., 2008. Failure of neuronal maturation in Alzheimer disease dentate gyrus. J. Neuropathol. Exp. Neurol. 67, 78–84.
Lin, M.T., Beal, M.F., 2006. Mitochondrial dysfunction and oxidative stress in neurodegenerative diseases. Nature 443, 787–795.
Lin, C.L., Cheng, Y.S., Li, H.H., Chiu, P.Y., Chang, Y.T., Ho, Y.J., Lai, T.J., 2016. Amyloid-beta suppresses AMP-activated protein kinase (AMPK) signaling and contributes to alpha-synuclein-induced cytotoxicity. Exp. Neurol. 275 (Pt 1), 84–98.
Lustbader, J.W., Cirilli, M., Lin, C., Xu, H.W., Takuma, K., Wang, N., Caspersen, C., Chen, X., Pollak, S., Chaney, M., Trinchese, F., Liu, S., Gunn-Moore, F., Lue, L.F., Walker, D.G., Kuppusamy, P., Zewier, Z.L., Arancio, O., Stern, D., Yan, S.S., Wu, H., 2004. ABAD directly links Abeta to mitochondrial toxicity in Alzheimer's disease. Science 304, 448–452.
Manczak, M., Calkins, M.J., Reddy, P.H., 2011. Impaired mitochondrial dynamics and abnormal interaction of amyloid beta with mitochondrial protein Drp1 in neurons from patients with Alzheimer's disease: implications for neuronal damage. Hum. Mol. Genet. 20, 2495–2509.
Morris, R., 1984. Developments of a water-maze procedure for studying spatial learning in the rat. J. Neurosci. Methods 11, 47–60.
Newman, D.J., Cragg, G.M., 2016. Natural products as sources of new drugs from 1981 to 2014. J. Nat. Prod. 79, 629–661.
Onyango, I.G., Dennis, J., Khan, S.M., 2016. Mitochondrial dysfunction in Alzheimer's disease and the rationale for bioenergetics based therapies. Aging Dis. 7, 201–214.
Pagani, L., Eckert, A., 2011. Amyloid-beta interaction with mitochondria. Int. J. Alzheimers Dis. 2011, 925050.
Pedros, I., Petrov, D., Allgaier, M., Sureda, F., Barroso, E., Beas-Zarate, C., Auladell, C., Pallas, M., Vazquez-Carrera, M., Casadesus, G., Folch, J., Camins, A., 2014. Early alterations in energy metabolism in the hippocampus of APPswe/PS1dE9 mouse model of Alzheimer's disease. Biochim. Biophys. Acta 1842, 1556–1566.
Puri, R., 2017. Protecting mitochondrial health: a unifying mechanism in adult neurogenesis. J. Neurosci. 37, 6603–6605.
Racioppi, L., Means, A.R., 2012. Calcium/calmodulin-dependent protein kinase kinase 2: roles in signaling and pathophysiology. J. Biol. Chem. 287, 31658–31665.
Rafalski, V.A., Brunet, A., 2011. Energy metabolism in adult neural stem cell fate. Prog. Neurobiol. 93, 182–203.
Schon, E.A., Przedborski, S., 2011. Mitochondria: the next (neurode)generation. Neuron 70, 1033–1053.
Shabestari, M.H., Meeuwenoord, N.J., Filippov, D.V., Huber, M., 2016. Interaction of the amyloid beta peptide with sodium dodecyl sulfate as a membrane-mimicking detergent. J. Biol. Phys. 42, 299–315.
Teng, L., Zhao, J., Wang, F., Ma, L., Pei, G., 2010. A GPCR/secretase complex regulates beta- and gamma-secretase specificity for Abeta production and contributes to AD pathogenesis. Cell Res. 20, 138–153.
Wang, X., Su, B., Perry, G., Smith, M.A., Zhu, X., 2007. Insights into amyloid-beta-induced mitochondrial dysfunction in Alzheimer disease. Free Radic. Biol. Med. 43, 1569–1573.
Wang, X., Su, B., Siedlak, S.L., Moreira, P.I., Fujioka, H., Wang, Y., Casadesus, G., Zhu, X., 2008. Amyloid-beta overproduction causes abnormal mitochondrial dynamics via differential modulation of mitochondrial fission/fusion proteins. Proc. Natl. Acad. Sci. U. S. A. 105, 19318–19323.
Wang, X., Su, B., Lee, H.G., Li, X., Perry, G., Smith, M.A., Zhu, X., 2009. Impaired balance of mitochondrial fission and fusion in Alzheimer's disease. J. Neurosci. 29, 9090–9103.
Wilkins, H.M., Swerdlow, R.H., 2016. Relationships between mitochondria and neuroinflammation: implications for Alzheimer's disease. Curr. Top. Med. Chem. 16, 849–857.
Won, J.S., Im, Y.B., Kim, J., Singh, A.K., Singh, I., 2010. Involvement of AMP-activated-protein-kinase (AMPK) in neuronal amyloidogenesis. Biochem. Biophys. Res. Commun. 399, 487–491.
Zhang, C.S., Hawley, S.A., Zong, Y., Li, M., Wang, Z., Gray, A., Ma, T., Cui, J., Feng, J.W., Zhu, M., Wu, Y.Q., Li, T.Y., Ye, Z., Lin, S.Y., Yin, H., Piao, H.L., Hardie, D.G., Lin, S.C., 2017. Fructose-1,6-bisphosphate and aldolase mediate glucose sensing by AMPK. Nature 548, 112–116.